Changing patterns of eastern Mediterranean shellfish exploitation in the Late Glacial and Early Holocene: Oxygen isotope evidence from gastropod in Epipaleolithic to Neolithic human occupation layers at the Haua Fteah cave, Libya

A.L. Prendergast a, *, R.E. Stevens [b], T.C. O'Connell [c], A. Fadlalak [d], M. Touati [e], A. al-Mzeine [d], [1], B.R. Schone [a], C.O. Hunt [f], G. Barker [c]

a Institute of Geosciences, Johann-Joachim-Becher-Weg 21, University of Mainz, 55128, Germany

b Institute of Archaeology, University College London, 31-34 Gordon Square, London, WC1H 0PY, United Kingdom

c McDonald Institute for Archaeological Research, University of Cambridge, Downing Street, Cambridge, CB2 3DZ, United Kingdom

d Department of Antiquities, Shahat, Cyrene, Libya

e Department of Archaeology, University of al-Beida, al-Beida, Libya

f Liverpool John Moores University, Liverpool, United Kingdom

Abstract

The seasonal pattern of shellfish foraging at the archaeological site of Haua Fteah in the Gebel Akhdar, Libya was investigated from the Epipaleolithic to the Neolithic via oxygen isotope ($\delta^{18}O$) analyses of the topshell *Phorcus (Osilinus) turbinatus*. To validate this species as faithful year-round palaeoenvironmental recorder, the intra-annual variability of $\delta^{18}O$ in modern shells and sea water was analysed and compared with measured sea surface temperature (SST). The shells were found to be good candidates for seasonal shellfish forging studies as they preserve nearly the complete annual SST cycle in their shell $\delta^{18}O$ with minimal slowing or stoppage of growth. During the terminal Pleistocene Early Epipaleolithic (locally known as the Oranian, with modeled dates of 17.2-12.5 ka at 2σ probability, Douka et al., 2014), analysis of archaeological specimens indicates that shellfish were foraged year-round. This complements other evidence from the archaeological record that shows that the cave was more intensively occupied in this period than before or afterwards. This finding is significant as the period of the Oranian was the coldest and driest phase of the last glacial cycle in the Gebel Akhdar, adding weight to the theory that the Gebel Akhdar may have served as a *refugium* for humans in North Africa during times of global climatic extremes. Mollusc exploitation in the Latest Pleistocene and Early Holocene, during the Late Epipaleolithic (locally known as the Capsian, *c.* 12.7 to 9 ka) and the Neolithic (*c*. 8.5 to 5.4 ka), occurred predominantly during winter. Other evidence from these archaeological phases shows that hunting activities occurred during the warmer months. Therefore, the timing of Holocene shellfish exploitation in the Gebel Akhdar may have been influenced by the seasonal availability of other resources at these times and possibly shellfish were used as a dietary supplement when other foods were less abundant.

1 Introduction

Molluscs have been a common dietary component for coastal populations throughout the world since the late Pleistocene (e.g. Marean, 2014). They are a predictable and easily obtainable food resource. They are also highly nutritious, containing abundant protein and essential micronutrients that are important for brain development and nervous system function and which are not as readily available from terrestrial resources (Erlandson, 2001; Broadhurst et al., 2002; Fa, 2008; Kyriacou et al., 2014). In the Mediterranean, mollusc shell remains are present in many archaeological sites from the Lower Palaeolithic to recent times (Colonese et al. 2011).

Analysing the chemistry of mollusc shells from archaeological sites allows the season in which the animal died to be determined and therefore provides information on the season of their harvesting. As molluscs generally precipitate their shells in oxygen isotopic equilibrium with ambient environmental conditions, the oxygen isotope composition of the last deposited shell portion is a reflection of the environmental conditions before the animal died (Epstein et al., 1951; Wefer and Berger, 1991). The oxygen isotope composition of marine shell is primarily controlled by water temperature and the oxygen isotope composition of seawater (Epstein et al., 1951; Wefer and Berger, 1991). In modern marine environments in mid to high latitudes, the role of evaporation and precipitation on the overall isotopic composition of seawater is negligible, permitting robust $\delta^{18}O$-derived sea surface temperature (SST) estimates. Warmer temperatures enrich ^{16}O relative to ^{18}O in the shell, to generate lower $\delta^{18}O$ values, whereas cooler temperatures produce higher $\delta18O$ values. If they grow shell during both seasonal extremes, molluscs of these habitats can record the full seasonal SST amplitude in their $\delta^{18}O$ values. Shackleton (1969, 1973) was the first to use oxygen isotope analysis to determine seasonal shellfish foraging patterns from archaeological sites. It has since been employed in many archaeozoological studies around the world (e.g. Bailey et al., 1983; Deith, 1986; Mannino et al., 2003, 2007; Colonese et al., 2009; Burchell et al., 2013a,b; Eerkens et al., 2013; see Andrus, 2011; Prendergast and Stevens, 2014 and Thomas, 2015 for recent reviews).

Seasonal patterns of shellfish collection bear directly upon interpretations of site use and subsistence behaviour, providing important data to aid analyses of foraging practices from the archaeological record (e.g. Bailey et al., 1983; Deith, 1986; Colonese et al., 2009; Mannino et al., 2007, 2011). These data can be combined with other archaeological data to gain a more complete picture of site use patterns throughout the year (e.g. Mannino et al., 2007). Epipaleolithic to Mesolithic shellfish foraging patterns have been elucidated from various archaeological sites in the Atlantic and Mediterranean regions (e.g. Mannino et al., 2003, 2007, 2011; Colonese et al., 2009). However, so far little attention has been paid to the southern Mediterranean and northern coast of Africa.

The Mediterranean archaeological site of Haua Fteah in north- eastern Libya (Fig. 1) contains a record of human occupation from at least marine isotope stage (MIS) 5 until the present day (McBurney, 1967; Barker et al., 2010, 2012; Douka et al., 2014). Subsistence evidence from the site includes a broad spectrum of marine and terrestrial resources including large and small mammals, reptiles, birds, wild plants and marine and terrestrial molluscs (McBurney, 1967; Klein and Scott, 1986; Barker et al., 2010, 2012) Shellfish, particularly the topshell *Phorcus turbinatus* and the limpet *Patella caerulea*, are abundant in the Late Glacial and Early Holocene (Hunt et al., 2011). Little is known about the seasonal use of resources at these times.

In this paper, we investigate the changing patterns of shellfish foraging during the Late Glacial and Early Holocene phases of occupation at the archaeological site of Haua Fteah, Libya. Because inter and intra-specific differences in growth rates, physiology, and environmental responses may cause deviations in the isotopic profiles of mollusc shells from equilibrium (Schone, 2008), the oxygen isotope variability in a modern *P. turbinatus* population in the intertidal zone closest to the archaeological site is examined to ensure that *P. turbinatus* oxygen isotopes reliably record local climatic conditions in the Gebel Akhdar. Then, oxygen isotope profiles from archaeological shells are characterised to detect whether shellfish formed a year-round resource or whether their collection was limited to specific seasons throughout the archaeological sequence. The shellfish foraging data are then compared with other subsistence data from Haua Fteah. Our results add important data in support of the hypothesis that the Gebel Akhdar served as a *refugium* for ancient human populations during times of climatic extremes in MIS 2 (Barker et al., 2012; Prendergast, 2013).

2 Setting

2.1 Environmental and archaeological setting

The Gebel Akhdar is a limestone massif in northeastern Libya that rises to a height of approximately 900 m above sea level (Fig. 1). The region is one of the few areas of high elevation along the North African coastline. As such, it attracts higher rainfall than surrounding areas and supports Mediterranean vegetation in contrast to the arid coastal corridors to the east and west, and the Sahara desert to the south (Hegazy et al., 2011).

Haua Fteah is the largest cave in the Gebel Akhdar region. It is interpreted to have formed as a phreatic cave in Tertiary limestone that subsequently partly collapsed (Barker et al., 2010). The cave lies near the foot of the Gebel Akhdar around 1 km inland from the Mediterranean at an elevation of approximately 60 m above sea level. The cave mouth measures approximately 20 m high and 80 m wide and faces towards the Mediterranean Sea. The site was originally excavated over three seasons in the 1950s to a depth of 14 m (McBurney, 1967). It is being re-excavated as part of the TRANS-NAP project at the University of Cambridge (Barker et al., 2008, 2009, 2010, 2012; Rabett et al., 2013; Farr et al., 2014). The TRANS-NAP excavations have reached Middle Palaeolithic units (Farr et al., 2014). Numerous smaller caves in the Gebel Akhdar have revealed evidence of late Pleistocene to Holocene human occupation and shellfish exploitation including Hajj Criem, Hagfet al Gama, and Hagfet et Dabba (Fig. 1, McBurney and Hey, 1955; Barker et al., 2009).

The marine shellfish assemblage in the Haua Fteah is dominated by the topshell *Phorcus turbinatus* and the limpet *Patella caerulea* (McBurney, 1967; Barker et al., 2010; Hunt et al., 2011). These species are also the most abundant shellfish on the modern shores of the Gebel Akhdar. They were present in the earliest occupational phases of the cave but did not become abundant until the Epi-palaeolithic (McBurney, 1967). This study focuses on *P. turbinatus* from the Late Glacial and Early Holocene (Epipalaeolithic to Neolithic) phases of human occupation at Haua Fteah as this species has a more consistent presence than *Patella caerulea* throughout the sequence (Hunt et al., 2011).

The Epipalaeolithic phase of occupation was divided into two cultural phases by McBurney (1967) (Fig. 1): the Oranian (his Layers XII-XV), approximately contemporaneous with and equivalent to the Iberomaurusian in the Maghreb; and the Libyco-Capsian (his Layers XI and X) with similarities to the Capsian of the Maghreb (hereafter referred to as the Capsian). The Oranian phase has been dated in a recent study to c. 17.2-12.5 ka cal. BP (at 2σ probability), i.e. to the period of deglaciation within MIS 2 following the Last Glacial Maximum (Douka et al., 2014). McBurney divided the assemblage into an Early phase (his Layers XV-XIV) in which reverse trimmed bladelets were relatively rare, and a Late phase (Layers XIII, XII) in which they were more abundant (McBurney, 1967). It has been suggested that the Gebel Akhdar might have served as a *refugium* for human populations during the Oranian/Late Glacial (Barker et al., 2010, 2012; Prendergast, 2013), because conditions in the cave at this time appear to have remained relatively humid compared to the hyperarid conditions that persisted in the coastal corridors to the east and west and in the Sahara desert to the south (Inglis, 2012; Prendergast, 2013) and that may have caused a contraction of MIS 2 populations into the Gebel Akhdar. The Latest Pleistocene to Early Holocene Capsian assemblage (Layers XI and X), dated to c. 12.5 ka to 7.9 ka cal. BP (at 2σ probability, Douka et al., 2014), is characterized by backed bladelets, true microliths, and increasing numbers of artefacts from bone and ostrich eggshell (McBurney, 1967).

The Neolithic assemblage in Layers VIII-VI, which has been dated from 8.5 to 5.4 ka cal. BP (at 2σ probability, Douka et al., 2014), is markedly different from the underlying assemblages (McBurney, 1967). These layers were characterized by the introduction of pottery, beads and painted pebbles and included pressure-flaked stone artefacts, hoe-shaped implements of limestone, grinding implements, bone artefacts, and ostrich eggshell as well as bones of domesticated sheep and goats (McBurney, 1967). There is currently no unambiguous evidence for crop domestication at this time. It appears that hunting and foraging continued to be practised alongside pastoralism (Barker et al., 2012).

Occupation density in the cave remained high (although with some fluctuations) throughout the Late Glacial and Early to Middle Holocene (McBurney, 1967; Barker et al., 2010, 2012). The presence of abundant shellfish along with other plant and animal resources including barbary sheep, gazelles, hartebeests, bovines, reptiles, land snails and wild plants attests to the broad spectrum diet

characteristic of many Epipaleolithic and Neolithic archaeological sites in the Mediterranean basin (Barker et al., 2009, 2012). During the Epipalaeolithic, shellfish exploitation was limited to intertidal species, the most common being *Phorcus turbinatus* and *Patella caerulea*. Several other species appear during the Neolithic (Hunt et al., 2011). Some shell beads are also present but they were most probably collected as rolled beach shells (Hunt et al., 2011).

2.2 *Phorcus (Osilinus) turbinatus*

P. turbinatus is a rocky shore species that inhabits the lower intertidal zone. It favours areas exposed to high wave energy with low salinity oscillations (Schifano and Censi, 1983; Mannino et al., 2008). *P. turbinatus* shells are composed of a thinner outer calcite layer and a thicker inner aragonite layer. Daily, fortnightly and annual growth increments and growth lines are clearly visible within the inner aragonite layers in cross section (Prendergast et al., 2013). Studies of modern populations in the Mediterranean have found strong correlations between shell $\delta^{18}O$ values and sea surface temperatures, indicating that this species is a reliable year- round palaeothermometer (Schifano and Censi, 1983; Mannino et al., 2008; Colonese et al., 2009; Prendergast et al., 2013). The species has successfully been used for season of collection studies in Italy (Mannino et al., 2008; Colonese et al., 2009). However, differences in growth rates and the timing of growth stops have been observed in different populations, in different habitats and at different latitudes (Regis, 1972; Schifano, 1983; Valli and Vio, 1975; Mannino et al., 2008; Prendergast et al., 2013). It is therefore necessary to examine the local modern populations in the Gebel Akhdar before reconstructing the season or seasons of collection at Haua Fteah.

3 Materials and methods

3.1 Modern and archaeological sample collection

Sea surface temperature (SST) measurements for Sousa during the study period were obtained from the advanced very high resolution radiometer (AVHRR) instrument (Table 1), a space-borne sensor that flies on the NOAA (National Oceanic and Atmospheric Administration) Polar Operational Environmental Satellites (POES) and the European MetOp Satellite. SST is measured using AVHRR's infrared channels. Satellite estimates of SST are made by converting the radiance measured in the infrared channels to brightness temperature and then using a multichannel technique to calculate SST to within $\pm 0.5\ ^0C$ (Kilpatrick et al., 2001). SST was obtained from the Pathfinder Version 5 project, which has reanalysed the AVHRR data to create global coverage at 4 km resolution (ftp://ftp. nodc.noaa.gov/pub/data.nodc/pathfinder). Monthly averages were used for this study.

To assess the modern inter-annual $\delta^{18}O_{shell}$ and $\delta^{18}O_{water}$ range along the Gebel Akhdar coastline, five live *P. turbinatus* specimens and one sea water sample were collected each month between February and September 2012 from the rocky intertidal zone east of Sousa about 1 km northwest of the Haua Fteah (Fig. 1, GPS location: 32.907994^0, 22.044392^0 WGS84). The original aim of the study was to collect samples over a 12 month period, but collection was cut short by the civil unrest in the region. As the continental shelf off the Gebel Akhdar is steep, changes in sea level during the last glacial cycle would not have greatly altered the horizontal distance of the Haua Fteah from the coast. However sea level regressions may have made some areas of coastline more cliffed, making access more difficult. The collection site at Sousa would have been one of the easiest locations for ancient inhabitants of the cave to collect live shellfish in antiquity as the site is a tidal platform which is shallowly inundated at high tide and offers a relatively flat path from the base of the Gebel Akhdar to the intertidal zone, in contrast to the many precipitous areas to the east and west where rock platforms are difficult to access. Care was taken that no air gap was left in the water sample collection bottles to avoid any isotopic exchange between the two phases that could have affected the isotope ratios of the water. Immediately after collection, the fish were frozen to avoid any additional shell growth. In the laboratory, bodies were removed with a dissecting needle, and organic material adhering to the shells was removed with a scalpel. The maximum basal diameter (MBD) and height of each shell (from outer lip to apex) was measured using digital calipers with an error of 0.1 mm (Appendix 1).

Additionally, five modern *P. turbinatus* shells live-collected during the summer of 1955 (McBurney, 1967) were also analysed to calibrate the season of collection methodology used in this study (Section 3.3).

Whole archaeological shells with intact edges were collected from archaeological layers in the Haua Fteah spanning the Oranian, Capsian and Neolithic phases of occupation, partly from the site and partly from the McBurney archive in Cambridge (Fig. 1). A minimum of 14 shells were analysed per archaeological unit.

Medium sized shells (around 20 mm MBD) were preferentially selected to avoid any inconsistencies in the data due to varied growth rates (e.g. Mannino et al., 2007). Shell samples from the TRANS-NAP excavations were picked from the archaeological assemblage after they had been sorted, counted and measured for the archaeomalacology component of the TRANS-NAP project (see Hunt et al., 2011). Further samples from the McBurney excavations were selected from the collection curated by the Museum of Archaeology and Anthropology, University of Cambridge (Appendix 2). X-ray diffraction (XRD) was used to determine whether any of the primary aragonite in the archaeological shells had altered to calcite as a result of diagenesis (Appendix 3). A total of 46 archaeological *P. turbinatus* were analysed from the cave (Table 3).

3.2 Pretreatment and drilling

To ensure comparability of results, shell pretreatment methods follow previous stable isotope studies of *P. turbinatus* (Mannino et al., 2007, 2008; Colonese et al., 2009; Prendergast et al., 2013). After cleaning with distilled water, whole modern and archaeological *P. turbinatus* shells were pretreated in a bath of 5% aqueous reagent-grade sodium hypochlorite at room temperature for 48 h to remove organic matter. After pretreatment, shells were rinsed in an ultrasonic bath for five minutes in distilled water three times before being oven-dried at $50\ ^0$ C for 12 h.

Pretreated *P. turbinatus* shells were sectioned across their outer whorl perpendicular to the direction of shell growth using a Buehler Isomet 1000 Precision Saw (Fig. 2). The lower part of the shell was mounted in Methyl ethyl ketone peroxide (MEKP) resin mixed with MEKP hardener and left to cure for 24 h. The section was then successively ground on 400, 600 and 1200 grit paper to remove any resin from the shell surface and then polished. Selected shells were stained with Feigl's solution (Feigl, 1958), which allows differentiation of aragonite from calcite. Aragonite is more soluble than calcite so if samples are left in the solution for 20 min, aragonite is stained grey whilst calcite remains unaffected (Feigl, 1958; Kato et al., 2003; Fenger et al., 2007). This allowed any diagenesis that may have occurred in the inner aragonite layers of the shells to be detected.

Samples for stable isotope analysis from both modern and archaeological shells were drilled from shell sections using a 0.3 mm drill bit mounted under a binocular microscope. Where sequential samples were taken along the axis of growth, sample spacing was approximately 0.6-0.9 mm. Sample weights ranged between 40 and 100 mg. All samples were drilled from the inner aragonite layer of the shells, with care taken to avoid any contamination with the outer calcite layer. The aragonite phase was analysed because it is easier to recognise growth increments than in the calcite layer, allowing greater sampling resolution; and because it is easier to detect diagenetic alteration to calcite in the aragonite phase via X-ray diffraction or by staining with Feigl's solution (Kato et al., 2003). This is particularly important when applying this methodology to the archaeological shells.

3.3 Season of collection methodology

In archaeological season of collection studies, high-resolution sequential $\delta^{18}O_{shell}$ analyses that cover the full annual range of $\delta^{18}O_{shell}$ variation allow the time of shell collection to be accurately determined (e.g. Hallmann et al., 2009). However, this method requires many $\delta^{18}O$ analyses from each shell, so limits the total number of individual shells that can be analysed in a particular study. To allow us to analyse a greater number of archaeological shells, and thereby detect more robust foraging patterns, we followed the method of Mannino et al. (2003) whereby the full annual $\delta^{18}O_{shell}$

range from at least one shell within each archaeological unit was used to approximate the range of possible $\delta^{18}O_{shell}$ values within that unit (Table 2). Then, for the remaining archaeological shells, short-sequences of three sequential $\delta^{18}O_{shell}$ samples were analysed inwards from the growing edge to characterise the $\delta^{18}O$ pattern of the most recent shell growth. The annual $\delta^{18}O_{shell}$ range was used to generate quartiles for each archaeological unit, which were then equated to the seasons (Fig. 2C): the lower quartile (<25%) reflects warm SSTs during summer; the upper quartile (>75%) reflects cool SSTs during winter; and the middle quartiles (25-75%) reflect intermediate SSTs during autumn or spring.

Short-sequence $\delta^{18}O_{shell}$ values are then used to determine in which quartile (therefore in which season) the shell died (Fig. 2C). For intermediate quartiles, the pattern of $\delta^{18}O_{shell}$ variation in the short-sequence samples allows the determination of whether the final months of shell growth were in a warming (spring) or a cooling (autumn) phase. This methodology offers a balance between analysing sufficient shells per archaeological unit to detect meaningful foraging patterns, and adequately characterising the pattern of growth to determine the season of collection. It has been successfully applied to detect seasonal foraging patterns from *P. turbinatus* shells in Italy (Mannino et al., 2007; Colonese et al., 2009).

Forty six archaeological shells from Oranian (n ¼ 16), Capsian (n ¼ 14) and Neolithic (n ¼ 16) layers were drilled using the short sequence method to characterize the season of collection. The annual oxygen isotope variation in these archaeological layers was characterized from the outer whorl of two Oranian, one Capsian and one Neolithic shell, with up to 72 samples analysed per shell (Fig. 4).

The season of collection methodology was validated for five modern shells from Sousa using the method of Mannino et al. (2003). For two of these shells (MRBO1 and MRBO3), samples were drilled along the whole outer whorl to characterize the annual $\delta18O_{shell}$ range at Sousa (Fig. 4A and B). The season of collection interpreted using this methodology was then compared to the actual season of collection (Table 3). Additionally, to test how well $\delta^{18}O_{shell}$ from modern *P. turbinatus* tracks SST, the outermost growth increment of one modern shell from each month of collection in Sousa was drilled (Fig. 2B) and the resultant $\delta^{18}O_{shell}$ curves were compared to monthly modern SST data (Fig. 3).

3.4 Stable isotope analysis

Oxygen isotope ratios from shell carbonate ($\delta^{18}O_{shell}$) were measured at the Godwin Laboratory, Department of Earth Sciences, University of Cambridge, England, and the Institute of Geosciences, University of Mainz, Germany. The samples were transferred to exetainer vials and sealed with silicone rubber septa using a screw cap. The samples were flushed with CP grade helium then acidified, left to react for 1-2 h at 70 ^{0}C and then analysed on a Thermo Finnigan MAT 253 continuous flow isotope ratio mass spectrometer, equipped with a Gas Bench II. Isotope data were calibrated against an NBS 19 calibrated in-house to the Carrara marble standard ($\delta^{18}O$ ¼ − 1.74‰) with 1σ external reproducibility and internal precision of 0.06‰. The results are reported with reference to the international standard VPDB.

Oxygen isotope ratios from sea water ($\delta^{18}O_{water}$) were measured at the Godwin Laboratory. Each sample was pre-filtered through 2.7 mm GF/D syringe filters to remove any particulate content, and then transferred to 2 ml Picarro autosampler vials. $\delta18O$ was measured by cavity ringdown laser spectroscopy (CRDS) using an L1102-iPicarro water isotope analyzer and A0211 high-precision vaporizer. Each batch of nine samples was analysed in conjunction with three standard waters that were used for calibration. Internal standards were calibrated against VSMOW, VGISP, and VSLAP. All results are reported in parts per mil (‰) relative to VSMOW. The precision is better than ±0.2‰ for $\delta^{18}O_{water}$ based on replicate analyses of laboratory standards.

Modern measured $\delta18O_{shell}$ was used to calculate SST using the empirically derived temperature equation for biogenic aragonite of Grossman and Ku (1986) with a scale correction by Gonfiantini et al. (1995) (see also Dettman et al., 1999; Sharp, 2007). The monthly measured value of $\delta^{18}O_{water}$

from Sousa was used in the equation:

$$SST^0C = 20.6 - 4.34(\delta^{18}O_{shell}(VPDB) - (\delta^{18}O_{water}(VSMOW) - 0.27)) \qquad (1)$$

Equation (1) was chosen as it has been found to accurately predict SST from *P. turbinatus* $\delta^{18}O_{shell}$ in other regions of the Mediterranean (e.g. Mannino et al., 2008; Colonese et al., 2009), whereas other marine aragonite palaeotemperature equations yielded higher offsets between measured and calculated SST in the same species (Mannino et al., 2008). The instrumental precision of ±0.1‰ is equivalent to an error of ±0.4 ^{0}C for SST calculated from $\delta^{18}O_{shell}$ using the Grossman and Ku (1986) equation.

Predicted $\delta^{18}O_{shell}$ was calculated using Equation (2), which is a rearrangement of Equation (1) to determine $\delta^{18}O_{shell}$. The measured month-by-month $\delta^{18}O_{water}$ values from Sousa were used in these calculations.

$$\delta^{18}O_{shell,predicted}=(20.6+4.34(\delta^{18}O_{water}(VSMOW)-0.27)-T)\times4.34^{-1} \quad (2)$$

3.5. Radiocarbon dating

To supplement the revised chronology established from various absolute dating methods by Douka et al. (2014), and to establish where the analysed shells fell within it, five of the *P. turbinatus* shells used for the season of collection analysis were dated using accelerator mass spectrometry (AMS) radiocarbon dating at the Oxford Radiocarbon Accelerator Unit, UK. These shells come from both the McBurney archive and the TRANS-NAP excavations (Appendix 4). The shells chosen for dating had well-preserved growth increments and did not show evidence of recrystallisation. The radiocarbon pretreatment and dating methods are described in Ramsey et al. (2004). Dates were calibrated using MARINE09 (Hughen et al., 2004; Reimer et al., 2009) and corrected for the global ocean radiocarbon reservoir (408 years) and the local Mediterranean radiocarbon reservoir of 58 ± 85 years (Reimer and McCormac, 2002). Calibrated ages are denoted as cal. BP.

4 Results

4.1 Modern data

Oxygen isotopes of marine water in Sousa ranged between þ1.0 and þ1.5‰ from February to September with a mean of þ1.0‰ (Table 1). AVHRR SST from Sousa ranged between 16.3 and 27.3 ^{0}C (Fig. 3B) with a mean annual SST of 22.0 ^{0}C and a range of 11.1 ^{0}C. The highest SSTs occurred in August and the lowest during February/March. There was a sharp rise in temperatures between April and July and a sharp fall in SST from October to February.

The measured $\delta^{18}O_{shell}$ edge values from Sousa ranged between -0.3‰ in August to þ2.2‰ in March (Table 1, Fig. 3A). SSTs calculated from these $\delta^{18}O_{shell}$ values using Equation (1) ranged between 15.3 ^{0}C and 25.2 ^{0}C (Table 1, Fig. 3B). These calculated SSTs closely track SST records from the AVHRR data (Table 1, Fig. 3B). The correlation between AVHRR SST and shell edge calculated SST was excellent (R^2 ¼ 0.977, Fig. 3E). The $\delta^{18}O_{shell}$ edge values predicted using Equation (2) are also highly correlated with measured $\delta18O_{shell}$ edge values (Fig. 3C and D, R^2 ¼ 0.983 when monthly varied values are used in the calculations and R^2¼0.976 for when mean annual $\delta^{18}O_{water}$ values are used).

The intra-annual $\delta^{18}O_{shell}$ ranges from sequential stable isotope samples drilled from the outer whorl of two modern shells collected from Sousa in 1955 are between -0.6 and þ2.0‰ for shell MRBO1 (mean ¼ þ0.6‰, range ¼ 2.6‰,n ¼ 46) and between -0.4 and þ2.3‰ for shell MBRO3 (mean ¼ þ0.9‰, range ¼ 2.7‰,n ¼ 71) (Table 2, Fig. 4A and B). Using the mean annual $\delta^{18}O_{water}$ value in

Equation (1), this corresponds to a calculated temperature range of 14.9 ^{o}C to 26.2 ^{o}C for shell MBRO1 (mean ¼ 21.1 ^{o}C, range ¼ 11.3 ^{o}C), and between 14.0 ^{0}C and 25.4 ^{0}C for shell MBRO3 (mean ¼ 19.8 ^{0}C, range ¼ 11.4 ^{0}C, Appendix 2). The three sequential $\delta^{18}O_{shell}$ edge values from the five live-collected modern shells from 1955 range between –O.2 and þ0.1‰. These all fall within the lower $\delta^{18}O$ quartile calculated from the modern Sousa shells, indicating summer season of death (Table 3).

4.2. Archaeological data

The five AMS radiocarbon ages obtained from the Haua Fteah *P. turbinatus* shells are shown in Table 3. The ages of the shells from layers assigned by McBurney to the Oranian (14169-13716, 15504-14277, and 14929-13941 cal. BP) all fall within the revised chronological range for the Oranian (17.2-12.5 ka: Douka et al., 2014). The age of the shell from an assumed Capsian context (14169-13716 cal. BP) is slightly older than the modeled age for the Capsian of 12.3 to 9.3 ka (Douka et al., 2014) and fits with other evidence that sedimentary recycling has mixed some Oranian and Capsian material (Hunt et al., 2015). The age for the Neolithic shell (7476-7126 cal. BP) falls within the 7.7 to 6.2 ka modelled range for the Neolithic (Douka et al., 2014).

The long-sequence $\delta^{18}O_{shell}$ samples from the outer whorls of the archaeological shells follow sinusoidal patterns with annual maximum and minimum values clearly visible (Fig. 4, Appendix 2). The $\delta18O_{shell}$ variation for each shell covers a full year of growth. The $\delta^{18}O_{shell}$ values of shells ascribed to the Oranian phase (Fig. 4C and D) are generally higher, indicating cooler SSTs during MIS 2. The $\delta^{18}O_{shell}$ values during the Capsian and Neolithic phases (Fig. 4E and F) are generally lower, indicating warmer SSTs during MIS 1, although changes in oceanic $\delta^{18}O$ because of changing sea levels would also be partially responsible for the changing $\delta^{18}O_{shell}$ values. However, more shells from each archaeological unit need to be analysed to provide robust reconstructions of MIS 2 to 1 SST variation in the Gebel Akhdar. This will be the focus of future research. In this study, the long-sequence $\delta^{18}O_{shell}$ profiles from the archaeological shells were used to characterize the likely annual range of $\delta^{18}O_{shell}$ values that may be found within each archaeological phase and to calculate quartile ranges for each archaeological unit. These quartile ranges were then used to interpret season of collection of the other shells within the same archaeological phase (Table 2, Fig. 2C).

The Late Glacial Oranian was the only archaeological unit where the $\delta^{18}O$ values of shell edges fall across all quartiles (Table 3). Thirteen out of fourteen Capsian $\delta^{18}O$ values of shell edges fall within the upper quartile (Table 3), whilst the remaining Capsian $\delta^{18}O_{shell}$ edge value falls within the lower quartile. The $\delta^{18}O$ values of shell edges for most (n ¼ 12) of the Neolithic shells analysed in this study fall within the upper quartile (Table 3). Two shells fall within the middle quartiles with their isotopic pattern showing a decreasing trend. None of the analysed Neolithic shells fall within the lower quartile.

5 Discussion

5.1 Modern isotope temperature comparisons

Measured and predicted $\delta^{18}O_{shell}$ from Sousa are highly correlated (Fig. 3C and D). This suggests that shell carbonate was precipitated in oxygen isotopic equilibrium with ambient seawater. SSTs calculated from $\delta^{18}O$ values of shell edges using Equation (1) (Fig. 3B) clearly track the monthly SST variations in the AVHRR SST data and are also highly correlated (Fig. 3E, R^2 ¼ 0.977). Similar correlations were found for *P. turbinatus* populations in Italy by Mannino et al. (2008, R^2 ¼ 0.75-0.91), Colonese et al. (2009, R^2 ¼ 0.91), and Schifano and Censi (1983) (R^2 ¼ 0.87) and in Malta by Prendergast et al. (2013, R^2 ¼ 0.96). These results confirm that *P. turbinatus* $\delta^{18}O_{shell}$ offers an excellent archive for both palaeothermometry and season of collection studies in the

Mediterranean and extend the application of this species as a palaeothermometer into the eastern Mediterranean basin.

To capture the full range of climatic variability in their chemical signatures, a shell needs to grow during both seasonal extremes. However, some studies of *P. turbinatus* have suggested that the animal ceases or significantly slows its growth at the hottest times of year and therefore preserves an attenuated record of seasonality (Schifano and Censi, 1983; Mannino et al., 2008; Colonese et al., 2009). Schifano and Censi (1983) and Mannino et al. (2008) observed annual growth lines in *P. turbinatus* in Sicily in late summer to early autumn, suggesting that the animals experienced at least a significant slowing of growth during summer when ambient SSTs exceeded their physiological tolerance. Temperatures above 25 ^{0}C have thus been suggested as a physiological limit for *P. turbinatus* at some sites (Shifano and Censi, 1983; Mannino et al., 2008; Colonese et al., 2009) whereby growth either stops or significantly slows so that samples for stable isotope analysis will be more time-averaged. The predicted $\delta^{18}O_{shell}$ from Libya under-estimated the measured $\delta^{18}O_{shell}$ values by ~0.5‰ between June and September (Fig. 3A). This equates to an offset between measured and calculated SST of around 2 ^{0}C. The study of Maltese populations found no such limitation: smaller-sized shells continued to record temperatures up to 27 ^{0}C (Prendergast et al., 2013). The negative offsets between instrumental and calculated SST for warmer months in the Sousa dataset may be related to the slower growth rates expected for the larger/older shells compared to the younger/smaller shells used in Malta (Prendergast et al., 2013). This should be borne in mind when selecting shells for season of collection analysis: if possible, larger/older shells should be avoided. The lowest SST recorded in the AVHRR SST data for northeast Libya was 16.3 ^{0}C. Calculated SSTs from Libya were 1 ^{0}C cooler than this, which is within the error margins of the technique. This shows that at least some *P. turbinatus* in Sousa continued to grow throughout the coldest times of year, thus providing a full lower range of SST seasonality.

The long $\delta^{18}O_{shell}$ sequences from the outer whorl of the two *P. turbinatus* shells collected in 1955 do record SSTs above 25 ^{0}C (Appendix 2). The $\delta^{18}O_{shell}$ profiles from these shells show relatively rounded peaks and troughs, suggesting that growth may not have substantially slowed during the summer for these animals (Fig. 4A and B). The $\delta^{18}O$ values of the shell edges for all five of the 1955-collected specimens were within the lower quartile for modern shells (Table 3). Therefore, summer death is interpreted for all these animals, which is consistent with their actual season of death (McBurney, 1967), showing that summer season of collection information can be obtained from *P. turbinatus* from Sousa.

5.2 Archaeological season of collection

The *P. turbinatus* $\delta^{18}O$ patterns from shell edges provide information on the seasonal shellfish foraging strategies from the different archaeological units of Haua Fteah. The presence of marine shellfish in conjunction with other archaeological material confirms the presence of humans at the site in particular seasons. This information can be used in conjunction with other evidence from the site to assess whether the cave was occupied year-round or seasonally. When patterns of shellfish foraging are studied in conjunction with other archaeological evidence for subsistence, such as macrobotanical and zooarchaeological remains, a more detailed picture of seasonal resource use through time can be built up.

5.2.1 Late Glacial (Oranian)

The Oranian was the only archaeological unit with evidence for *P. turbinatus* harvesting during all four seasons. There was a fairly even spread of shellfish foraging activities across the seasons with five shells harvested during autumn, three in winter, four in spring and four in summer (Table 3, Fig. 5). This implies that during the Late Glacial, the cave was used year-round rather than on a seasonal basis. From the season of collection analysis alone it is not possible to determine whether this

represents permanent occupation at the site or episodic visits throughout the year. However, in combination with other evidence from the archaeological record it seems likely that the Oranian represented a more permanent occupation. The lithic, shell and bone assemblages from this part of the cave stratigraphy are all much more numerous than in other phases of occupation, and evidence for more trampling damage on bone fragments from Oranian layers compared to in the succeeding Early Holocene (Capsian) layers also suggests more intensive occupation, at least in the excavated part of the cave (Barker et al., 2010). The frequency of core residues and micro-debitage indicates that the cave was used for a range of activities that required in situ use and reshaping of finished blades (Barker et al., 2012). There was also a significant increase in the abundance of marine and terrestrial molluscs at this time compared with in underlying archaeological units (McBurney, 1967; Barker et al., 2010; Hunt et al., 2011). Increased exploitation of marine resources is commonly associated with intensification of foraging activities and lower mobility (Binford, 2001; Nadel, 2004). The exploitation of molluscs in all seasons at the Haua Fteah in the Late Glacial could therefore point to increased mollusc consumption and high resource pressure, with the Gebel Akhdar supporting a denser and less mobile foraging population.

Palaeoenvironmental reconstructions from land snail stable isotopes (Prendergast, 2013) and soil micromorphology (Inglis, 2012) have shown that the Oranian use of the cave was during the coldest and driest phase of the Late Glacial in the Gebel Akhdar. However, although the climate of the Gebel Akhdar at this time was relatively cold and dry, it was not as harsh as in the surrounding regions (Inglis, 2012; Prendergast, 2013), suggesting that the massif formed a buffer to the climatic extremes experienced in surrounding coastal lowlands and desert areas. This finding adds weight to the theory that the Gebel Akhdar may have served as a *refugium* for humans in North Africa during times of global climatic extremes such as MIS 2 (e.g. Barker et al., 2008, 2010; Prendergast, 2013), especially given evidence for a decline in population densities elsewhere in North Africa and the Levant at this time (e.g. Ambrose, 1998; Cremaschi, 1998). Additionally, the changing glacio-eustatic sea levels at this time may have exposed shoreline freshwater springs (e.g. Faure et al., 2002) that would also have enhanced the attractiveness of this region for human populations.

5.2.2 Latest Pleistocene to Early Holocene (Capsian)

Thirteen of the fourteen Capsian $\delta^{18}O_{shell}$ edge values fall within the upper quartile (Table 3), indicating that with the transition to the Holocene *P. turbinatus* were foraged almost exclusively in winter. Other fauna from Capsian contexts included low quantities of fish and crab and the continued presence of barbary sheep (*Ammotragus*), gazelle and hartebeest (Barker et al., 2010) along with birds that were possibly exploited year-round (MacDonald, 1987). Preliminary bone fusion data from large mammals in Capsian layers indicated that sub-adult individuals were hunted in preference to adults (Barker et al., 2010), possibly an indicator that hunting activities were focused towards the summer/autumn months when juveniles were present in the landscape. Luminance analysis of *Ammotragus* teeth from Capsian contexts indicates the predominantly summer exploitation of these large caprids (Wall-Scheffler, 2007). Cone-scales of *Pinus halepensis* suggest that pine cones were gathered in the summer and then later opened by heating adjacent to fires (J.Morales, pers.comm.). Other plant foods also amenable for storage such as wild pulses and legumes, and seeds or berries of shrubs or small trees such as juniper (*Juniperus phoenicea*), the mastic tree (*Pistacia lentiscus*), and myrtle (*Myrtus communis*) were likely collected in summer. Capsian artefacts found in the Gebel Akhdar uplands point to a wide-ranging use of the landscape during the Latest Pleistocene to Early Holocene, possibly as result of seasonal foraging expeditions (Barker et al., 2010). In short, the shellfish season of collection data chime with other indicators suggesting a shift towards settled foraging with increased seasonality in foraging activities, presumably in response to shifts in resource availability.

These findings are in line with early Holocene shellfish foraging patterns elsewhere in the Mediterranean, which show that shell- fish were predominantly collected during cooler months (Mannino et al., 2007, 2014; Colonese et al., 2009). In southwestern Italy, Colonese et al. (2009) found that early Holocene *P. turbinatus* from several Mesolithic sites were foraged almost exclusively

in the colder and intermediary seasons. At Grotta dell'Uzzo in north- western Sicily, *P. turbinatus* were collected predominantly during autumn and winter during the early Mesolithic, whereas in the later Mesolithic, shellfish foraging occurred throughout the year, possibly associated with ritual feasting (Mannino et al., 2007). At Grotta d'Oriente, almost all shellfish were collected during the cooler months during the early and late Mesolithic use of the cave, even when shellfish foraging intensified in the later Mesolithic (Mannino et al., 2014). This cooler season shellfish exploitation in Italy has been suggested to have been a response to the seasonal availability of other dietary resources, particularly large mammals such as red deer (e.g. Colonese et al., 2009), and the same may have been the case at the Haua Fteah, though it cannot be discounted that cooler season collection may also have been governed by taste, as the taste and texture of shellfish varies throughout the year, particularly when they spawn around spring/summer (Mannino et al., 2008).

5.2.3 Neolithic

The $\delta^{18}O$ values of shell edges for most of the shells from the Neolithic layers analysed in this study fall within the upper quartile (Table 3), indicating that shellfish foraging predominantly occurred in winter. Two shells fall within the middle quartiles with their isotopic pattern showing a warming trend, indicating autumn collection. None of the analysed Neolithic shells were collected in the warmer months of the year. During this period, shellfish exploitation increased in dietary importance at the Haua Fteah on the evidence of both the number of shellfish remains present at the site and the species diversity (Barker et al., 2012). Notably, though, the mean size of specimens diminished in the earliest Neolithic, suggesting unsustainable levels of exploitation (Hunt et al., 2011). The increase in shellfish exploitation was accompanied by the exploitation of a wide range of botanical and faunal resources and the appearance of domesticated caprids (McBurney, 1967; Barker et al., 2012). No evidence for domesticated crops has been found in the Haua Fteah Neolithic sequence (Barker et al., 2012). It seems the Neolithic inhabitants of Haua Fteah continued to rely on wild resources including plants, shellfish and large mammals even after the introduction of domesticated animals. All Neolithic *P. turbinatus* were collected in the autumn or winter. In the Mediterranean, winter is a time of reduced resource availability (e.g. Mannino et al., 2011). As in the Capsian, shellfish may have been used to supplement the diet during sparser times of the year when other resources were less available.

Studies of shellfish foraging elsewhere in the Mediterranean have also noted that the appearance of Neolithic material culture was accompanied by an intensification of mollusc exploitation (Mannino et al., 2007, 2014; Colonese et al., 2009, 2014). In the Grotta d'Oriente in southern Italy, for example, although some early Neolithic shellfish foraging occurred throughout the year, the majority occurred in cooler seasons (Mannino et al., 2014). At Grotta dell'Uzzo in northwestern Sicily, in the early Neolithic, molluscs were mainly collected during winter with minor collection in autumn and spring, whilst in the late Neolithic molluscs were collected in all seasons coincident with an increase in human occupation evidence in the cave (Mannino et al., 2007).

It is noteworthy that with the introduction of domestic cereals and/or animals to different parts of the Mediterranean alongside the spread of Neolithic material culture, shellfish foraging frequently continued and in some cases intensified. The low primary productivity of the Mediterranean zone, however, limits the secondary biomass available on Mediterranean shores (Fa, 2008). This means that molluscs probably never provided a major dietary source of protein for late Pleistocene and Holocene populations in the Mediterranean as they did in the North Atlantic (Bailey and Flemming, 2008; Fa, 2008). This can be seen from stable isotope analyses of bone collagen from various Mediterranean archaeological sites, which generally suggest little or no marine food consumption (e.g. Paine et al., 2009; Craig et al., 2010; Lightfoot et al., 2011; Mannino et al., 2011, 2012). Although, regional variability exists as at some sites in the western Mediterranean, the contribution of marine resources to the diet at this time is estimated to be as high as 25% (Guixe' et al., 2006). Intertidal molluscs would have provided essential micronutrients not readily available from other dietary resources (Erlandson, 2001; Broadhurst et al., 2002; Fa, 2008; Kyriacou et al., 2014), and would have provided an important dietary supplement when other protein sources were less readily available. It seems

likely that throughout the Mediterranean, shellfish foraging continued in the Neolithic as part of a broader year-round subsistence strategy.

6 Conclusion

This study has shown that $\delta^{18}O_{shell}$ from modern *P. turbinatus* shells is deposited in isotopic equilibrium with ambient environmental conditions and can be used to reconstruct local SST. Analysis of the $\delta^{18}O_{shell}$ of the last formed shell portion can be used reliably to reconstruct the season of death of the animal, thus providing data on the archaeological season of collection. These data can be combined with other subsistence data from the archaeological site to provide a seasonally constrained picture of site use. This study provides the first evidence for seasonal shellfish foraging from the Gebel Akhdar. The evidence presented here suggests that a shift in patterns of shellfish exploitation occurred during the Epipalaeolithic at the Haua Fteah. During the Late Glacial Oranian, *P. turbinatus* were exploited during every season in roughly equal numbers. This correlates with increased abundance of shellfish remains at the site as well as increased evidence for occupation density compared to underlying archaeological units. This year-round exploitation occurred at a time when regional climate was more arid. At this time the Gebel Akhdar remained relatively more humid and it is likely that people were able to survive there, as it became a *refugium* from surrounding environmental extremes. During the Latest Pleistocene and early to middle Holocene, the period of the Capsian Epipalaeolithic and Neolithic, *P. turbinatus* were collected predominantly during cooler seasons. Their collection may have been a part of an annual subsistence strategy linked to the seasonal availability of large mammal and wild plant resources.

References

Ambrose, S.H., 1998. Late Pleistocene human population bottlenecks, volcanic winter, and differentiation of modern humans. Journal of Human Evolution 34, 623-651.

Andrus, C.F.T., 2011. Shell midden sclerochronology. Quaternary Science Reviews 30, 2892-2905.

Bailey, G.N., Flemming, N.C., 2008. Archaeology of the continental shelf: marine resources, submerged landscapes and underwater archaeology. Quaternary Science Reviews 27, 2153-2165.

Bailey, G.N., Deith, M.R., Shackleton, N.J., 1983. Oxygen isotope analysis and seasonality determinations: limits and potential of a new technique. American Antiquity 48, 390-398.

Barker, G., Basell, L., Brooks, I., Burn, L., Cartwright, C., Cole, F., Davison, J., Farr, L., Grun, R., Hamilton, R., Hunt, C., Inglis, R., Jacobs, Z., Leitch, V., Morales, J., Morley, I., Morley, M., Pawley,

S., Stimpson, C., Twati, M., van der Veen, M., 2008. The Cyrenaican Prehistory Project 2008: the second season of investigations of the Haua Fteah cave and its landscape, and further results from the initial (2007) fieldwork. Libyan Studies 39, 175-221.

Barker, G., Antoniadou, A., Barton, H., Brooks, I., Candy, I., Drake, N., Farr, L., Hunt, C.O., Ibrahim, A., Inglis, R., Jones, S., Morales, J., Morley, I., Mutri, G., Rabett, R., Reynolds, T., Simpson, D., Twati, M., White, K., 2009. The Cyrenaican Prehistory Project 2009: the third season of investigations of the Haua Fteah cave and its landscape, and further results from the 2007-2008 fieldwork. Libyan Studies 40, 1-42.

Barker, G., Antoniadou, A., Armitage, S.J., Brooks, I., Candy, I., Connell, K., Douka, K., Farr, L., Hill, E., Hunt, C.O., Inglis, R., Jones, S., Lane, C., Lucarini, G., Meneely, J., Morales, J., Mutri, G., Prendergast, A.L., Rabett, R., Reade, H., Reynolds, T., Russell, N., Simpson, D., Smith, B., Stimpson, C., Twati, M., White, K., 2010. The Cyrenaican Prehistory Project 2010: the fourth season of investigations of the Haua Fteah cave and its landscape, and further results from the 2007-2009 fieldwork. Libyan Studies 41, 63-88.

Barker, G., Bennett, P., Farr, L., Hill, E., Hunt, C.O., Lucarini, G., Morales, J., Mutri, G., Prendergast, A.L., Pryor, A., Rabett, R., Reynolds, T., Spry-Marques, P., Twati, M., 2012. The Cyrenaican Prehistory Project 2012: the fifth season of investigation of the Haua Fteah cave. Libyan Studies 43, 1-22.

Binford, L.R., 2001. Constructing Frames of Reference: an Analytical Method for Archaeological Theory Building Using Ethnographic Datasets. University of California Press, Berkeley.

Broadhurst, C., Wang, Y., Crawford, M., Cunnane, S., Parkington, J., Schmidt, W., 2002. Brain-specific lipids from marine, lacustrine, or terrestrial food resources: potential impact on early African Homo sapiens. Comparative Biochemistry and Physiology 131, 653-673.

Burchell, M., Cannon, A., Hallmann, N., Schwarcz, H.P., Schone, B.R., 2013a. Inter-site variability in the season of shellfish collection on the Central Coast of British Columbia. Journal of Archaeological Science 40, 626-636.

Burchell, M., Hallmann, N., Martindale, A., Cannon, A., Schone, B.R., 2013b. Seasonality and intensity of shellfish harvesting in the north coast of British Columbia. Journal of Coastal and Island Archaeology 8, 152-169.

Colonese, A.C., Troelstra, S., Ziveri, P., Martini, F., Vetro Lo, D., Tommasini, S., 2009. Mesolithic shellfish exploitation in SW Italy: seasonal evidence from the oxygen isotopic composition of *Osilinus turbinatus* shells. Journal of Archaeological Science 36, 1935-1944.

Colonese, A.C., Mannino, M.A., Bar-Yosef Mayer, D.E., Fa, D., Finlayson, J.C., Lubell, D., Stiner, M.C., 2011. Marine mollusc exploitation in Mediterranean prehistory: an overview. Quaternary International 239, 86-103.

Colonese, A.C., Lo Vetro, D., Martini, F., 2014. Holocene coastal change and intertidal mollusc exploitation in the central Mediterranean: variations in shell size and morphology at Grotta d'Oriente (Sicily). Archaeofauna 23, 181-192.

Craig, O.E., Biazzo, M., Colonese, A.C., Di Giuseppe, Z., Martinez-Labarga, C., Lo Vetro, D., Lelli, R., Martini, F., Rickards, O., 2010. Stable isotope analysis of Late Upper Palaeolithic human and faunal remains from Grotta del Romito (Cosenza), Italy. Journal of Archaeological Science 37, 2504-2512.

Cremaschi, M., 1998. Late Quaternary geological evidence for environmental changes in south western Fezzan (Libyan Sahara). In: Hasan, F.A. (Ed.), Droughts, Food and Culture pp. 13-48. Springer, Amsterdam.

Deith, M., 1986. Subsistence strategies at a Mesolithic camp site: evidence from stable isotope analyses of shells. Journal of Archaeological Science 13, 61-78.

Dettman, D.L., Reische, A.K., Lohmann, K.C., 1999. Controls on the stable isotope composition of seasonal growth bands in aragonitic fresh-water bivalves (Unionidae). Geochimica et Cosmochimica Acta 63, 1049-1057.

Douka, K., Grün, R., Jacobs, Z., Lane, C., Farr, L., Hunt, C.O., Inglis, R., Reynolds, T., Albert, P., Aubert, M., Cullen, V., Hill, E., Kinsley, L., Roberts, R.G., Tomlinson, E.L., Wulf, S., Barker, G., 2014. The chronostratigraphy of the Haua Fteah cave (Cyrenaica, northeast Libya). Journal of Human Evolution 66, 39-63.

Eerkens, J.W., Byrd, B.F., Spero, H.J., Fritschi, A.K., 2013. Stable isotope reconstructions of shellfish harvesting seasonality in an estuarine environment: implications for late Holocene San Francisco Bay settlement patterns. Journal Archaeological Science 40, 2014-2024.

Epstein, S., Buchsbaum, R., Lowenstam, H., Urey, H.C., 1951. Carbonate-water isotopic temperature scale. Geological Society of America Bulletin 62, 417.

Erlandson, J.M., 2001. The archaeology of aquatic adaptations: paradigms for a new millennium. Journal of Archaeological Research 9, 287-350.

Fa, D.A., 2008. Effects of tidal amplitude on intertidal resource availability and dispersal pressure in prehistoric human coastal populations: the Mediterranean-Atlantic transition. Quaternary Science Reviews 27, 2194-2209.

Farr, L., Lane, R., Abdulazeez, F., Bennett, P., Holman, J., Marasi, A., Prendergast, A., Al-Zweyi, M., Barker, G., 2014. The Cyrenaican Prehistory Project 2013: the seventh season of excavations in the Haua Fteah cave. Libyan Studies 45, 163-173.

Faure, H., Walter, R.C., Grant, D.R., 2002. The coastal oasis: ice age springs on emerged continental shelves. Global and Planetary Change 33, 47-56.

Feigl, F., 1958. Spot Tests in Inorganic Analysis. Elsevier, Amsterdam.

Fenger, T., Surge, D., Schone, B., Milner, N., 2007. Sclerochronology and geochemical variation in limpet shells (*Patella vulgata*): a new archive to reconstruct coastal sea surface temperature. Geochemistry Geophyics Geosystems 8. Q07001.

Gonfiantini, R., Stichler, W., Rozanski, K., 1995. Standards andintercomparison materials distributed by the international atomic energy agency for stable isotope measurements. In: Reference and Intercomparison Materials for Stable Isotopes of Light Elements. I.A.E.A., Vienna. IAEA Technical Document 825, pp. 13-29.

Grossman, E.L., Ku, T.L., 1986. Oxygen and carbon isotope fractionation in biogenic aragonite: temperature effects. Chemical Geology 59, 59-74.

Guixe, E.G., Richards, M.P., Subira', M.E., 2006. Palaeodiets of humans and fauna at the Spanish Mesolithic site of El Collado. Current Anthropology 47, 549-556.

Hallmann, N., Burchell, M., Schone, B.R., Irvine, G.V., Maxwell, D., 2009. High-resolution sclerochronological analysis of the bivalve mollusk *Saxidomus gigantea* from Alaska and British Columbia: techniques for revealing environmental archives and archaeological seasonality. Journal of Archaeological Science 36, 2353-2364.

Hegazy, A.K., Boulos, L., Kabiel, H.F., Sharashy, O.S., 2011. Vegetation and species altitudinal distribution in Al-Jabal Al-Akhdar landscape, Libya. Pakistan Journal of Botany 43, 1885-1898.

Hughen, K.A., Baillie, M.G.L., Bard, E., Beck, J.W., Bertrand, C.J.H., Blackwell, P.G., Buck, C.E., Burr, G.S., Cutler, K.B., Damon, P.E., Edwards, R.L., Fairbanks, R.G., Friedrich, M., Guilderson, T.P., Kromer, B., McCormac, G., Manning, S., Ramsey, C.B., Reimer, P.J., Reimer, R.W., Remmele, S., Southon, J.R., Stuiver, M., Talamo, S., Taylor, F.W., van der Plicht, J., Weyhenmeyer, C.E., 2004. Marine04 marine radiocarbon age calibration, 0-26 cal kyr BP. Radiocarbon 46, 1029-1058.

Hunt, C.O., Reynolds, T.G., El-Rishi, H.A., Buzaian, A., Hill, E., Barker, G.W., 2011. Resource pressure and environmental change on the North African littoral: Epipalaeolithic to Roman gastropods from Cyrenaica, Libya. Quaternary International 244, 15-26.

Hunt, C.O., Gilbertson, D.D., Hill, E.A., Simpson, D., 2015. Sedimentation, resedimentation and chronologies in archaeologically-important caves: problems and prospects. Journal of Archaeological Science 56, 109-116.

Inglis, R., 2012. Human Occupation and Changing Environments during the Middle to Later Stone Ages: Soil Micromorphology at the Haua Fteah, Libya (Unpublished PhD Dissertation). Department of Archaeology and Anthropology, University of Cambridge.

Kato, K., Wada, H., Fujioka, K., 2003. The application of chemical staining to separate calcite and aragonite minerals for micro-scale isotopic analyses. Geochemical Journal Japan 37, 291-297.

Kilpatrick, K.A., Podesta, G.P., Evans, R., 2001. Overview of the NOAA/NASA advanced very high resolution radiometer Pathfinder algorithm for sea surface temperature and associated matchup database. Journal of Geophysical Research 106, 9179.

Klein, R., Scott, K., 1986. Re-analysis of faunal assemblages from the Haua Fteah and other Late Quaternary archaeological sites in Cyrenaican Libya. Journal of Archaeological Science 13, 515-542.

Kyriacou, K., Parkington, J.E., Marais, A.D., Braun, D.R., 2014. Nutrition, modernity and the archaeological record: coastal resources and nutrition among Middle Stone Age hunter-gatherers on the Western Cape coast of South Africa. Journal of Human Evolution 77, 64-73.

Lightfoot, E., Boneva, B., Miracle, P.T., Slaus, M., O'Connell, T.C., 2011. Exploring the Mesolithic and Neolithic transition in Croatia through isotopic investigations. Antiquity 85, 73-86.

MacDonald, K.C., 1987. The avifauna of the Haua Fteah (Libya). Archaeozoologia 9, 83-102.

Mannino, M.A., Spiro, B.F., Thomas, K.D., 2003. Sampling shells for seasonality: oxygen isotope analysis on shell carbonates of the inter-tidal gastropod *Monodonta lineata* (da Costa) from populations across its modern range and from a Mesolithic site in southern Britain. Journal of Archaeological Science 30, 667-679.

Mannino, M., Thomas, K., Leng, M., Piperno, M., Tusa, S., Tagliacozzo, A., 2007. Marine resources in the Mesolithic and Neolithic at the Grotta dell'Uzzo (Sicily): evidence from isotope analyses of marine shells. Archaeometry 49, 117-133.

Mannino, M., Thomas, K., Leng, M., Sloane, H., 2008. Shell growth and oxygen isotopes in the topshell *Osilinus turbinatus*: resolving past inshore sea surface temperatures. Geo-Marine Letters 28, 309-325.

Mannino, M.A., Thomas, K.D., Leng, M.J., Di Salvo, R., Richards, M.P., 2011. Stuck to the shore? Investigating prehistoric hunter-gatherer subsistence, mobility and territoriality in a Mediterranean coastal landscape through isotope analyses on marine mollusc shell carbonates and human bone collagen. Quaternary International 244, 88-104.

Mannino, M.A., Catalano, G., Talamo, S., Mannino, G., DiSalvo, R., Schimmenti, V., Lalulez, C., Messina, A., Petruso, D., Carameli, D., Richards, M.P., Sineo, L., 2012. Origin and diet of the prehistoric hunter-gatherers on the Mediterranean island of Favignana (Ergadi Islands, Sicily). PloS One 7 (11), e49082.

Mannino, M.A., Thomas, K.D., Crema, E.R., Leng, M.J., 2014. A matter of taste? Mode and periodicity of marine mollusc exploitation on the Mediterranean island of Favignana (Egadi Islands, Italy) during its isolation in the early Holocene. Archaeofauna 23, 133-147.

McBurney, C.B.M., 1967. The Haua Fteah (Cyrenaica) and the Stone Age of the South-East Mediterranean. Cambridge University Press, Cambridge.

McBurney, C., Hey, R.W., 1955. Prehistory and Pleistocene Geology in Cyrenaican Libya: a Record of Two Seasons' Geological and Archaelogical Fieldwork in the Gebel Akhdar Hills. Cambridge University Press, Cambridge.

Marean, C.W., 2014. The origins and significance of coastal resource use in Africa and Western Eurasia. Journal of Human Evolution 77, 17-40.

Nadel, D., 2004. The Ohalo II and the Natufian dwelling structures (Jordan Valley, Israel). In: Delage, C. (Ed.), The Last Hunter-Gatherer Societies in the Near East. British Archaeological Reports International Series, Oxford, pp. 137-151.

Paine, C., O'Connell, T., Miracle, P.T., 2009. Stable isotopic reconstruction of Early Mesolithic diet at Pupicina Cave. In: McCartan, S., Schulting, R., Warren, G., Woodman, P. (Eds.), Mesolithic Horizons. Oxbow Books, Oxford, pp. 210-216.

Prendergast, A.L., 2013. Late Pleistocene to Holocene Human-environment Interaction in the Southeastern Mediterranean: Stable Isotope Analysis of Mollusc Shells from Haua Fteah, Libya and Ksar Akil, Lebanon (Unpublished PhD Dissertation). Department of Archaeology and Anthropology, University of Cambridge.

Prendergast, A.L., Stevens, R.E., 2014. Molluscs (Isotopes): Analyses in Environmental Archaeology. The Encyclopaedia of Global Archaeology. Springer, Berlin, pp. 5010-5019.

Prendergast, A.L., Azzopardi, M., O'Connell, T.C., Hunt, C., Barker, G., Stevens, R.E., 2013. Oxygen isotopes from *Phorcus (Osilinus) turbinatus* shells as a proxy for sea surface temperature in the central Mediterranean: a case study from Malta. Chemical Geology 345, 77-86.

Rabett, R., Farr, L., Hill, E., Hunt, C., Lane, R., Moseley, H., Stimpson, C., Barker, G., 2013. The Cyrenaican prehistory project 2012: the sixth season of excavations in the Haua Fteah cave. Libyan Studies 44, 113-125.

Ramsey, C.B., Higham, T., Leach, P., 2004. Towards high-precision AMS; progress and limitations. Radiocarbon 46, 17-24.

Regis, M.B., 1972. Etude comparee de la croissance des Monodontes (Gasteropodes Prosobranches) en Manche et le long des cotes atlantiques et mediterraneennes françaises. In: Battaglia, B. (Ed.), Proceedings of the 5th European Marine Biology Symposium. Piccin, Padova, pp. 59-267.

Reimer, P.J., McCormac, F.G., 2002. Marine radiocarbon reservoir corrections for the Mediterranean and Aegean Seas. Radiocarbon 44, 159-166.

Reimer, P.J., Baillie, M.G.L., Bard, E., Bayliss, A., Beck, J.W., Blackwell, P.G., Ramsey, C.B., Buck, C.E., Burr, G.S., Edwards, R.L., Friedrich, M., Grootes, P.M., Guilderson, T.P., Hajdas, I., Heaton, T.J., Hogg, A.G., Hughen, K.A., Kaiser, K.F., Kromer, B., McCormac, F.G., Manning, S.W., Reimer, R.W., Richards, D.A., Southon, J.R., Talamo, S., Turney, C.S.M., van der Plicht, J., Weyhenmeyer, C.E., 2009. IntCal09 and Marine09 radiocarbon age calibration curves, 0-50,000years cal. BP. Radiocarbon 51, 1111-1150.

Sharp, Z., 2007. Principles of Stable Isotope Geochemistry. Pearson, New Jersey.

Schifano, G., 1983. Allometric growth as influenced by environmental temperature in *Monodonta turbinata* shells. Palaeogeography Palaeoclimatology Palaeoecology 44, 215-222.

Schifano, G., Censi, P., 1983. Oxygen isotope composition and rate of growth of *Patella coerulea*, *Monodonta turbinata* and *M. articulata* shells from the western coast of Sicily. Palaeogeography Palaeoclimatology Palaeoecology 42, 305-311.

Schone, B., 2008. The curse of physiology challenges and opportunities in the interpretation of geochemical data from mollusk shells. Geo-Marine Letters 28, 269-285.

Shackleton, N.J., 1973. Oxygen isotope analysis as a means of determining season of occupation of prehistoric midden sites. Archaeometry 15, 133-141.

Shackleton, N.J., 1969. Marine mollusca in archaeology. In: Brothwell, D., Higgs, E.S. (Eds.), Science in Archaeology. Thames and Hudson, London, pp. 407-414.

Thomas, K., 2015. Molluscs emergent, part 1: themes and trends in the scientific investigation of mollusc shells as resources for archaeological research. Journal of Archaeological Science 56, 133-140.

Valli, G., Vio, E., 1975. Studio di alcuni fattori che condizionano l'attivita di *Monodonta turbinata* (Born) (Gastropoda: Prosobranchia) ad Aurisina (Trieste). Bollettino Pesca Pisciolt Idrobiol 30, 127-134.

Wall-Scheffler, C., 2007. Digital cementum luminance analysis and the Haua Fteah hominins: how seasonality and season of use changed through time. Archaeometry 49, 815-826.

Wefer, G., Berger, W., 1991. Isotope paleontology: growth and composition of extant calcareous species. Marine Geology 100, 207-248.

FIGURES

Fig. 1. A: Locality of the study area (rectangle expanded in B) within the Mediterranean as well as other sites mentioned in the text, B: Inset from A, the study area in detail. Location of the Haua Fteah the modern collection site in Sousa and other archaeological sites mentioned in the text, C: Stratigraphy of the Haua Fteah based on the north facing section. Roman numerals in brackets next to the archaeological phases refer to the archaeological layers defined by McBurney (1967). Ages for each archaeological unit are from Douka et al. (2014) at 2σ probability. Stratigraphy drawn by L. Farr.
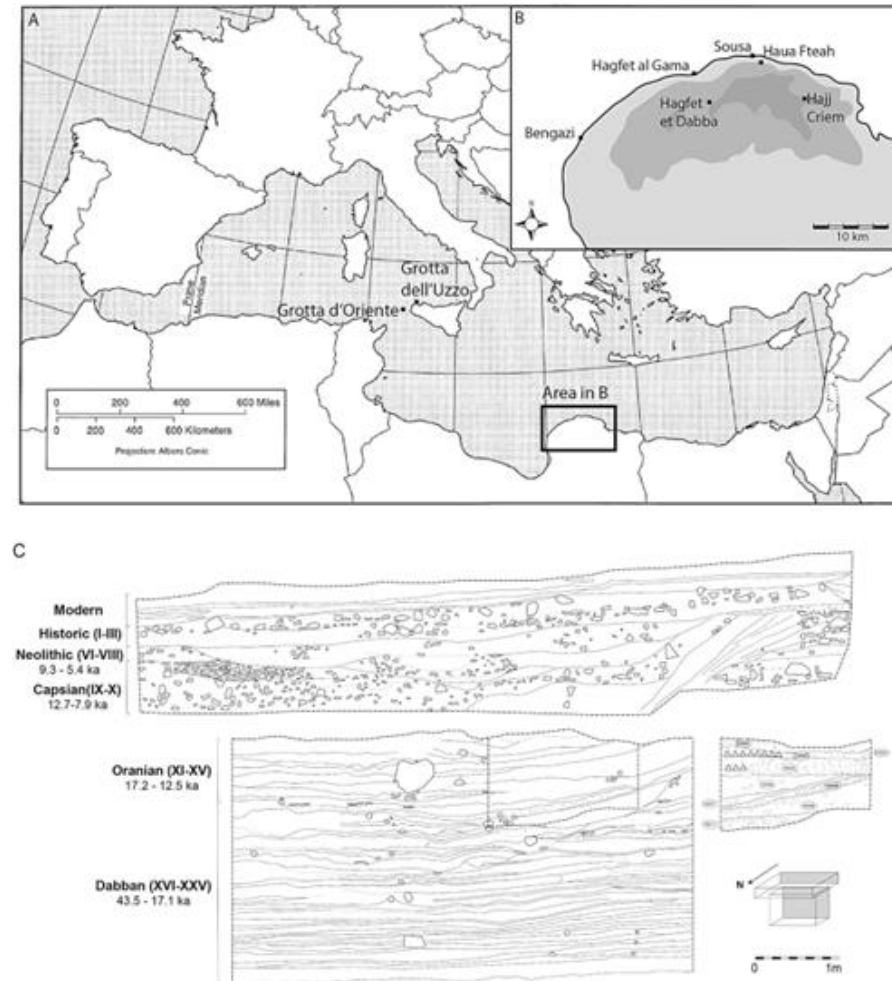
Fig. 2. Sampling shell and determination of quartiles. A: Schematic figure of a P. turbinatus shell showing the major morphological elements and the measurements of shell height and maximum basal diameter (Appendix 1). The dashed line shows the location of the cross section in B, B: Schematic cross section of the outer whorl of a *P. turbinatus* shell showing the major morphological features and the location of the outer increment stable isotope sample. DOG = direction of growth, C: Determination of season of collection from oxygen isotope quartiles of the annual range
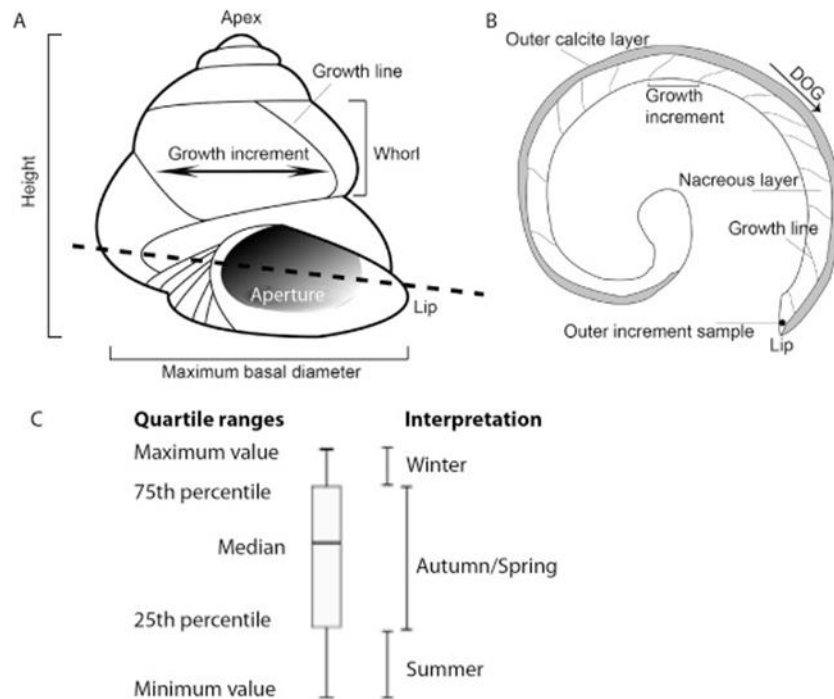
Fig. 3. SST and shell $\delta^{18}O$ values from modern shells. A: Month by month variation of measured δ18O values of shell edges (black circles); predicted $\delta^{18}O$ values of shell edges using Equation (2) and the AVHRR SST data for Sousa and monthly collected $\delta^{18}O_{water}$ values (triangles); and predicted $\delta^{18}O$ values of shell edges using Equation (2) and the AVHRR SST data for Sousa and the mean annual $\delta^{18}O_{water}$ value (diamonds), B: SST calculated using Equation (1) from monthly collected $\delta^{18}O_{water}$ values and $\delta^{18}O$ values of shell edges from monthly-collected shells (circles) compared to AVHRR SST (triangles). C and D: Correlation between measured $\delta^{18}O$ values of shell edges and predicted $\delta^{18}O$ values of shell edges using monthly-collected $\delta^{18}O_{water}$ values (D), and the mean annual $\delta^{18}O_{water}$ value (E), E: Correlation between $\delta^{18}O_{shell\ edge}$ calculated SST and AVHRR SST. All error bars are one standard deviation.
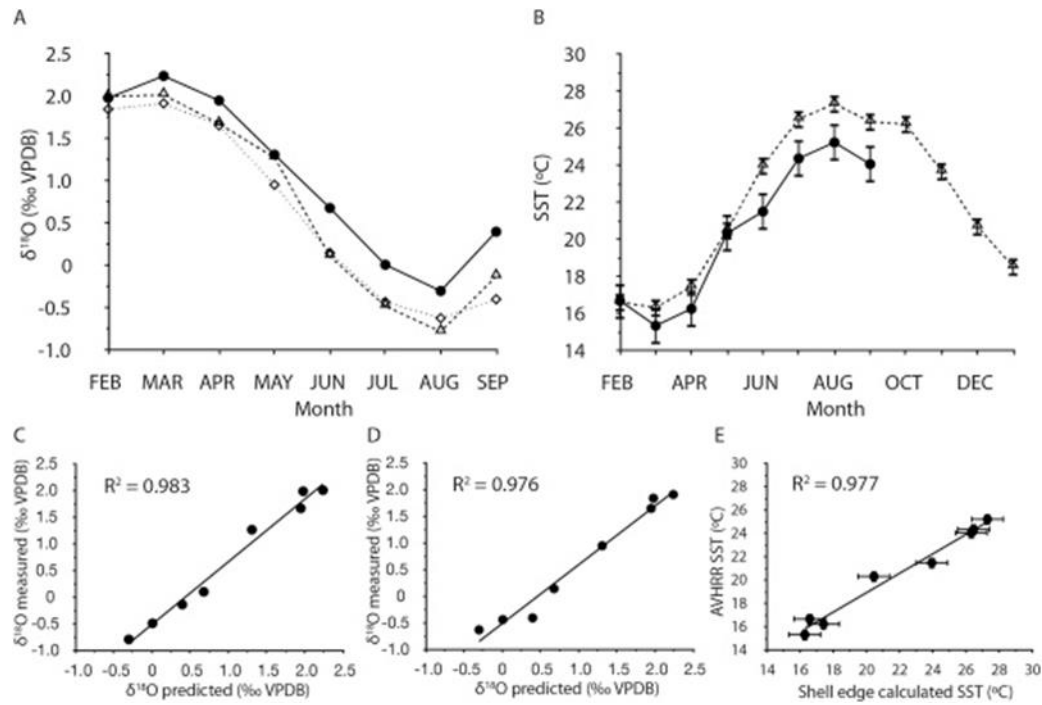
Fig. 4. Sequentially sampled $\delta^{18}O_{shell}$ sequences from the outer whorl of modern (A and B) and archaeological *P. turbinatus* shells from Oranian (C and D), Capsian (E), and Neolithic (F) units.

A Modern

B Modern

C Oranian

D Oranian

E Capsian
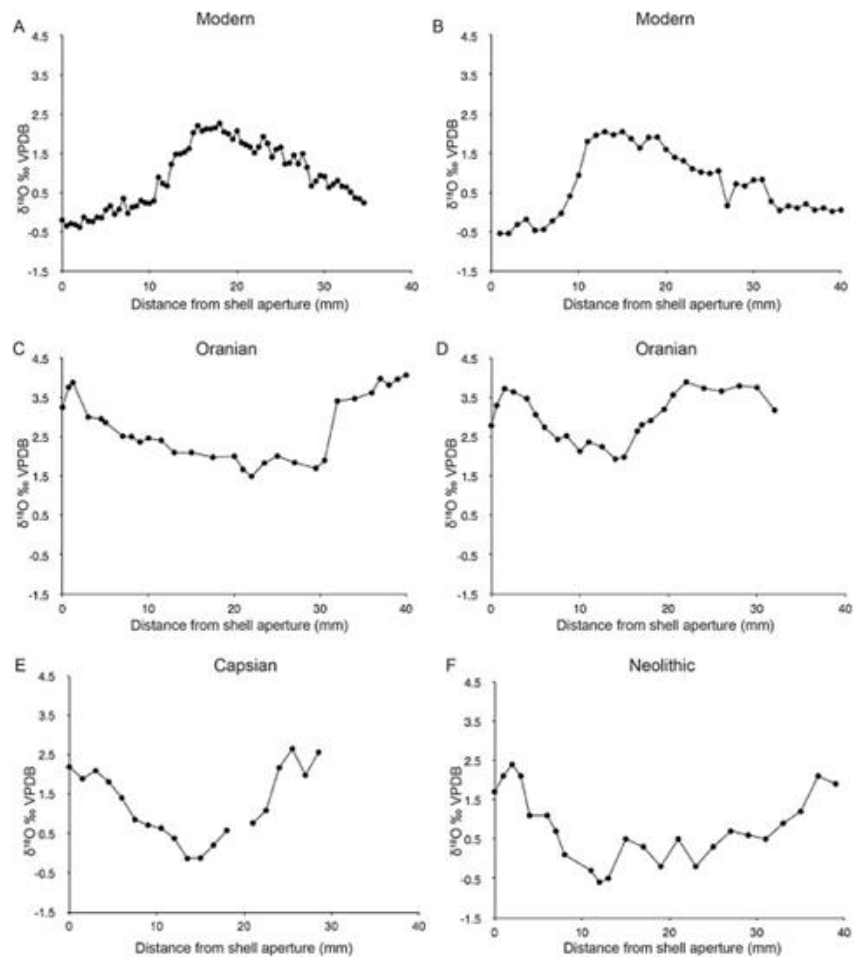
F Neolithic

Fig. 5. Pie charts and frequency distribution plots of the season of collection data based on $\delta^{18}O$ values of shell edges: (A) modern (B) Oranian (C) Capsian and (D) Neolithic shells. Pie charts are based on the interpretations presented in Table 3. Frequency distribution plots are of the outermost $\delta^{18}O_{shell}$ edge values plotted within the characterised $\delta^{18}O_{shell}$ range from each archaeological unit.
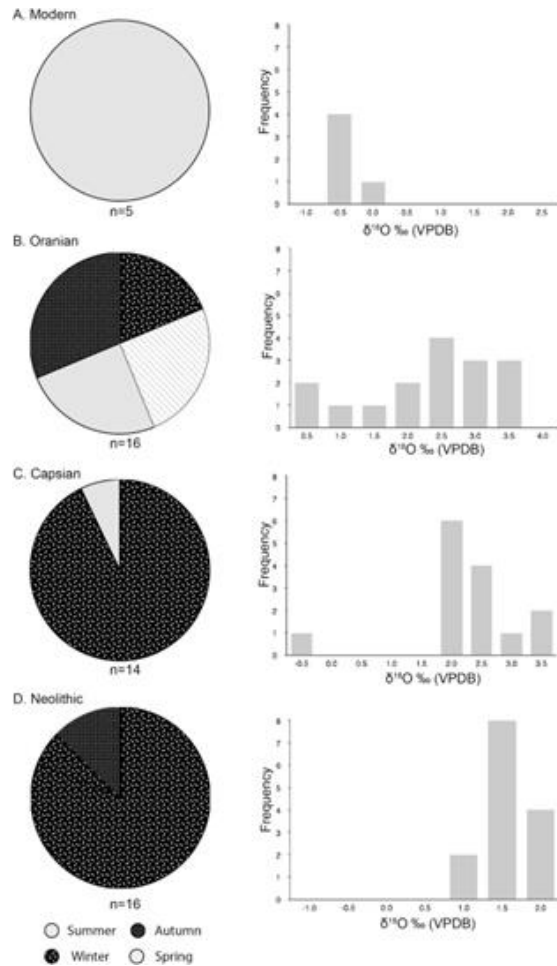
TABLES

Table 1. Modern $\delta^{18}O_{water}$ (‰ VSMOW), outer edge $\delta^{18}O_{shell}$ (‰ VPDB) and SST results from Sousa. SST data from the AVHRR satellite are provided and compared with SST calculated from $\delta^{18}O_{shell}$, and $\delta^{18}O_{water}$ using Equation (1). SST measurements are all expressed in °C.

Collection month	$\delta^{18}O_{water}$ ‰	$\delta^{18}O_{shell}$ ‰	Calculated SST[a] °C	Calculated SST[b] °C	AVHRR SST °C	Difference between measured and calculated SST[a]	Difference between measured and calculated SST[b]
February	+1.4	+2.0	16.7	16.5	16.6	0.1	0.1
March	+1.3	+2.2	15.3	15.3	16.3	1.0	1.0
April	+1.2	+2.0	16.3	16.6	17.5	1.2	0.8
May	+1.5	+1.3	20.3	19.4	20.5	0.2	1.1
June	+1.2	+0.7	21.5	22.1	24.0	2.5	1.9
July	1.2	+0.0	24.4	25.0	26.5	2.1	1.5
August	+1.0	−0.3	25.2	26.4	27.3	2.1	1.0
September	+1.5	+0.4	24.1	23.3	26.4	2.3	3.0
MEAN	+1.0	+1.0	20.5	20.6	21.9	1.4	1.3

a Calculated from outer shell edge $\delta^{18}O$ and monthly measurements of sea water $\delta^{18}O$ from Sousa using Equation (1).

b Calculated from outer shell edge $\delta^{18}O$ and mean annual sea water $\delta^{18}O$ of 1.3‰ from Sousa using Equation (1).

Table 2. Quartile ranges calculated from sequentially sampled *P. turbinatus* $\delta^{18}O_{shell}$ values over at least a year of growth. Where long $\delta^{18}O_{shell}$ sequences from more than one shell per archaeological unit are given, the combined data are used to generate quartiles and these are used for season of collection determinations presented in Table 3. For the complete isotopic dataset see Appendix 2.

Sample	Unit	Minimum value	25% quartile	50% quartile	75% quartile	Maximum value	Range
MBRO1	Modern	−0.6	−0.0	+0.3	+1.3	+2.0	2.6
MBRO3	Modern	−0.4	−0.2	+0.8	+1.6	+2.3	2.7
Modern combined	Modern	−0.6	−0.1	+0.7	+1.6	+2.3	2.9
AROC747G	Neolithic	−0.6	+0.1	+0.6	+1.6	+2.4	3.0
AROC01S3B	Capsian	−0.1	+0.6	+1.1	+2.0	+2.6	2.7
AROC05S5A	Oranian	+1.5	+2.0	+2.5	+3.5	+4.1	2.6
AROC06S1A	Oranian	+1.9	+2.5	+3.1	+3.7	+3.9	2.0
Oranian combined	Oranian	+1.5	+2.2	+2.8	+3.6	+4.1	2.6

Table 3. Season of collection data and new radiocarbon age determinations presented by archaeological unit: The quartiles (defined in Table 2) are used as the basis to interpret the season of the mollusc's death. When short-sequence $\delta^{18}O_{shell}$ edge values are within the lower quartile (<25%) summer death is interpreted, when they are within the upper quartile (>75%) winter death is interpreted, and for the intermediate quartiles (25%–75%) autumn or winter death is interpreted. The trend in the short-sequence $\delta^{18}O_{shell}$ for intermediate quartiles is used to determine autumn (cooling trend) or spring (warming trend) death. Stable isotope values are in VPDB. x = sample lost in mass spectrometer, na = unable to determine shell edge pattern. *$\delta^{18}O_{shell}$ edge value falls outside the range determined for its corresponding archaeological unit.

Culture	Sample ID	Sample 3 δ18O	Sample 2 δ18O	Edge δ18O	Quartile	Pattern	Trend	Season	Radiocarbon age (cal. BP)
Modern	MBRO1955-2	−0.5	−0.2	−0.1	Lower	Ascending	Cooling	Summer	
	MBRO1955-3	−0.3	0.1	0.1	Lower	Ascending	Cooling	Summer	
	MBRO1955-4	−0.2	−0.2	−0.1	Lower	Ascending	Cooling	Summer	
	MBRO1955-5	−0.4	−0.1	−0.2	Lower	Ascending	Cooling	Summer	
	MBRO1955-6	−0.3	−0.5	−0.1	Lower	Ascending	Cooling	Summer	
Neolithic	MBO1503S3B	2.2	2.1	2.1	Upper	Descending	Warming	Winter	
	MBO1503S3C	1.4	1.7	1.6	Upper	Ascending	Cooling	Winter	
	MBO1503S3D	2.3	2	1.9	Upper	Descending	Warming	Winter	
	MBO1503S3E	1.5	1.5	1.8	Upper	Ascending	Cooling	Winter	
	AROS747UC	2.5	2.6	+2.7*	Upper	Ascending	Cooling	Winter	
	AROS747UE	0.2	1.7	1.4	Intermediate	Ascending	Cooling	Autumn	
	AROS747UF	1.5	1.8	2.3	Upper	Ascending	Cooling	Winter	
	AROS747UH	1.3	1.6	1.9	Upper	Ascending	Cooling	Winter	
	AROS747UI	2.5	2.4	2.4	Upper	Ascending	Cooling	Winter	
	AROS747UJ	0.9	1.6	1.8	Upper	Ascending	Cooling	Winter	
	AROS747UK	1.2	1.7	1.6	Upper	Ascending	Cooling	Winter	
	AROS747UL	2.2	2.7	2.7	Upper	Ascending	Cooling	Winter	
	AROS747UG	2.4	2.1	1.7	Upper	Descending	Warming	Winter	
	AROS743UB	−1.7	1.6	1.7	Upper	Ascending	Cooling	Winter	
	AROS743UE	1.1	1.4	1.3	Intermediate	Ascending	Cooling	Autumn	
	AROS37A	2.6	2.9	2	Upper	Descending	Warming	Winter	7476–7126
Capsian	AROC01S3B	2.1	1.9	2.2	Upper	Ascending	Cooling	Winter	
	AROC01S2A	3.1	3.1	+3.2*	Upper	Ascending	Cooling	Winter	
	AROC01S2B	3	3.4	+3.5*	Upper	Ascending	Cooling	Winter	14169–13716
	AROC01S3A	1.3	1.7	2	Upper	Ascending	Cooling	Winter	
	AROC01S3C	x	3.8	+3.6*	Upper	Descending	Warming	Winter	
	AROC01S1C	1.6	2.5	2.6	Upper	Ascending	Cooling	Winter	
	AROC01S1B	2.4	2.8	2.7	Upper	Ascending	Cooling	Winter	
	AROC01S1M	−0.1	−0.1	−0.1	Lower	Level	Level	Summer	
	AROC01S1N	1.8	2.1	2.4	Upper	Ascending	Cooling	Winter	
	AROC01S1H	2	2.4	2.5	Upper	Ascending	Cooling	Winter	
	AROC01S1I	2.8	2.7	2.6	Upper	Descending	Warming	Winter	
	AROC01S1J	0.8	1.3	2.3	Upper	Ascending	Cooling	Winter	
	AROC01S1K	0.3	1.3	2	Upper	Ascending	Cooling	Winter	
	AROC01S1L	2.2	2	2	Upper	Descending	Warming	Winter	
Oranian	ARO10005A	3.9	3.8	3.2	Intermediate	Descending	Warming	Spring	
	AROC06S1A	3.6	3.7	3.3	Intermediate	Descending	Warming	Spring	

AROC06S1D	1.2	x	0.8	Lower	Descending	Warming	Summer	14857–13809
AROC06S2A	2.9	3.2	3.7	Upper	Ascending	Cooling	Winter	
AROC06S3A	3.1	2.2	2.9	Intermediate	Ascending	Cooling	Spring	
AROC06S4A	2.3	2.8	3.9	Upper	Ascending	Cooling	Winter	
AROC06S5A	3	3.5	3.9	Upper	Ascending	Cooling	Winter	
MBO1704S22A	2.2	2.4	2.8	Upper	Ascending	Cooling	Winter	14929–13941
AROC08S1A	0.5	0.7	0.8	Lower	Ascending	Cooling	Summer	
AROC08S1C	x	x	1.8	Lower	na	na	Summer	
AROC08S2B	0.6	0.9	2.2	Intermediate	Ascending	Cooling	Autumn	15504–14277
AROC08S3B	3	3.6	2.8	Intermediate	Descending	Warming	Spring	
AROC09S7A	2.8	2.8	3	Intermediate	Ascending	Cooling	Autumn	
AROC09S7C	1.3	1.9	2.7	Intermediate	Ascending	Cooling	Autumn	
AROS11011A	2.8	2.8	2.3	Intermediate	Descending	Warming	Spring	
AROS11015A	1.1	1.1	1.4	Lower	Ascending	Cooling	Summer	